ChemComm

Accepted Manuscript

This article can be cited before page numbers have been issued, to do this please use: X. Yu, S. Pan, K. Li, L. Li, M. Li, L. Shi and Y. Liu, *Chem. Commun.*, 2018, DOI: 10.1039/C8CC01031E.

ROYAL SOCIETY OF CHEMISTRY

rsc.li/chemcomm

View Article Online
DOI: 10.1039/C8CC01031E

Journal Name

COMMUNICATION

A reaction-based ratiometric fluorescent sensor for detection of Hg(II) ions both in cells and bacteria†

Received 00th January 20xx,
Accepted 00th January 20xx

DOI: 10.1039/x0xx00000x

www.rsc.org/

Sheng-Lin Pan, Kun Li,* Ling-Ling Li, Meng-Yang Li, Lei Shi, Yan-Hong Liu and Xiao-Qi Yu*

A novel reaction-based fluorescent probe (ATC-Hg) was designed and synthesized via "covalent assembly" principle, which exhibtied excellent selectivity and high sensitivity for Hg^{2+} and CH_3Hg^+. Moreover, it is the first Hg(II) senstive fluorescent probe that has been succesfully applied in imaging in both cells and *Escherichia coli*.

Mercury (Hg) is one of the most hazardous and ubiquitous heavy metals. Its bioaccumulation involves inorganic mercury (Hg^0, Hg^{2+}) and methylmercury species ($MeHg^+$), which can enter the food chain and are subsequently ingested by humans.[1] Because of high reactivity and liposolubility, Hg^{2+} and $MeHg^+$ can cause grisly immunotoxic, genotoxic, and neurototoxic effects, which can lead to many severe health problems such as kidney failure, central nervous system damage with various cognitive and motor disorders, and even death.[2] The increasing mercury contamination in our living environment and ecosystem has created significant concerns and thus its facile detection and effective tracing in biological samples is highly demanded. Owing to the high spatiotemporal resolution, sensitivity and selectivity, as well as simple operation procedures, fluorescence imaging has been regarded as one of the most effective and convenient method for detecting and sensing of Hg (II) and related compounds.

In recent years, various Hg^{2+} fluorescent probes based on the coordination with heteroatom-containing ligands have been reported.[3] However, these Hg(II) sensitive probes usually showed low selectivity due to theirs reversible complexation and the interferences from other metal cations (such as Ag^+, Cu^{2+}, Pb^{2+}, Fe^{2+} and Fe^{3+} ions et. al) [3a-g], or anions (like I^-, CN^- and PO_4^{3-} et. al) [3f-h] and other ligands (like dithiouracil, EDTA et. al) [3i]. By contrast, the irreversible reaction-based probes are advantageous in terms of selectivity and sensitivity, as they utilize a specific chemical reaction between a probe molecule and targeted species, which leads to the formation of a fluorescent or coloured product accompanied with a unique spectroscopic change. Moreover, this characteristic makes the design of ratiometric sensors easier. Since they allow the measurement of emission intensities at two different wavelengths, and are not easily disturbed by microenvironment, sensor concentration, photobleaching and excitation intensity, etc.[4, 5] Till now, most of the reported reaction-based Hg(II) probes have limitations including unsatisfactory water solubility,[5, 6] long response time,[5d-e, 6f] or high detection limit [5d-e, 6g, 7]. On the other hand, in contrast to inorganic mercury (Hg^{2+}) detection, only a few probes have been investigated as potential $MeHg^+$ sensors till now.[6d, 8] What's more, no probe has realized the imaging of Hg(II) both in cells and bacteria. Herein, we designed and synthesized a reaction-based ratiometric fluorescent probe **ATC-Hg** for Hg^{2+} and $MeHg^+$ detection in aqueous solutions. Importantly, for the first time, we further successfully applied **ATC-Hg** in the detection of Hg(II) both in Hela cells and *Escherichia coli*.

Through consulting literatures, we found the vast majority of Hg(II) sensitive fluorescent probes are designed based on Hg(II)-induced spirolactam ring-opening process of rhodamine derivatives (Scheme 1a), adopting the affinity of sulfur or selenium to Hg^{2+} ions.[1] Driven by desulfation or deselenization, mercury induces spirolactam ring open. Following that, coordination, hydrolysis or cyclization will happen, thus leading to the change of fluorescent signal. However, this sensing mechanism is only suitable for fluorescence intensity-enhanced probes rather than ratiomateric probes. Recently, Yang group reported a "covalent assembly" strategy to design Hg(II) probes, which utilize substrate-triggered chemical cascade reaction to furnish the conjugative backbone of a push-pull fluorescent dye.[6d-e] However, those probes have not been used in biological sample detection.[6d]

Our group have developed many reaction-based coumarin derivatives as florescent probes for ROS (reactive oxygen species), RSS (reactive sulphur species) and pH.[9] In light of "covalent assembly" strategy, we report a novel coumarin

[a] Key Laboratory of Green Chemistry and Technology, Ministry of Education, College of Chemistry Sichuan University, 29, Wangjiang Road, Chengdu, Sichuan Province. E-mail: kli@scu.edu.cn; xqyu@scu.edu.cn.

† Electronic Supplementary Information (ESI) available: [detail synthesis and experiment procedure, additional spectra (Uv-vis and fluorescence titration spectra, NMR and ESI-MS)]. See DOI: 10.1039/x0xx00000x

View Article Online
DOI: 10.1039/C8CC01031E

based fluorescent probe **ATC-Hg**, its performance in biological samples is also investigated. The key design strategy of **ATC-Hg** is the ortho 2-aminophenyl group installed to the Hg^{2+}/$MeHg^{+}$-reactive 1,3-dithiolane moiety, which causes the fluorescence change of coumarin derivatives through an ICT (intramolecular charge transfer) process. Once 1,3-dithiolane is desulfurized to a formyl group (**c-a**), a condensation with the nearby amino group (NH_2) will then occur to generate the product **c-ql**. It is a heterocyclic aromatic compound with larger conjugate planes than that of its precursor. In addition, NH_2 can coordinate to the mercury centre and thereby brings it in close proximity to 1,3-dithiolane, which is benefit for the intramolecular cyclocondensation reaction.

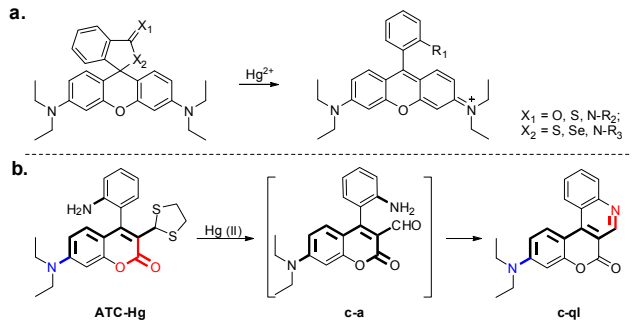

Scheme 1 a. The reported design strategy via Hg(II)-induced spirolactam ring-opening process; b. the "covalent assembly" mechanism for Hg(II) in this work.

Probe **ATC-Hg** was easily synthesized and characterized by NMR and HRMS (Scheme S1, ESI). As shown in Fig. 1, the spectral properties of **ATC-Hg** were studied in PBS buffer (10 mM, pH 7.4). It had a maximum absorption and emission at 405 nm and 492 nm, respectively. After reacted with Hg^{2+} completely, it showed a maximum absorption and emission at 480 nm and 572 nm, respectively. The quantum yields of **ATC-Hg** and **c-ql** in PBS buffer (10 mM, pH 7.4) were 0.7% and 9.3%, respectively. In consideration of better ratiometric effect and potential biological application of probe **ATC-Hg**, we chose 405nm as the optimum excitation wavelength.

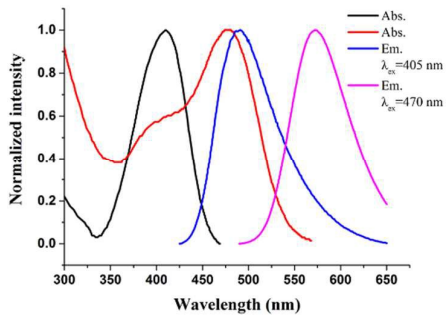

Fig. 1 Absorption and emission spectra of **ATC-Hg** before (black and blue) and after (red and pink) reacting with Hg^{2+} in PBS buffer (10 mM, pH 7.4). Slit: 5 nm/5 nm.

Then the responding activities were investigated. Upon addition of an aliquot of Hg^{2+} or $MeHg^{+}$ to **ATC-Hg** (5 μM) in PBS buffer solution (10 mM, pH 7.4), an emission peak at 572 nm appeared, while the emission at 492 nm from **ATC-Hg** decreased (Fig. 2a, 2b), which is in agreement with the expected conversion of **ATC-Hg** to **c-ql** (Scheme 1b). Meanwhile, an absorption band at 480 nm appeared, while the absorption at 410 nm from **ATC-Hg** decreased in UV-Vis spectra (Fig. S1, ESI), which was consistent with the variation tendency of fluorescence spectra.

The detection kinetics of **ATC-Hg** was also investigated. (Fig. S2, ESI) It showed that the reaction between **ATC-Hg** and Hg^{2+} can be completed within 3 min. On the other hand, the response sensitivity of $MeHg^{+}$ by **ATC-Hg** was much weaker than that of Hg^{2+}. After about 30 min, the reaction between **ATC-Hg** and $MeHg^{+}$ reached equilibrium.

Remarkably, the fluorescent intensity ratios at 572 and 492 nm (I_{572}/I_{492}) exhibited a drastic change from 0.25 (in the absence of Hg^{2+}) to 6.04 (in the presence of 1 eq. Hg^{2+}), a 24-fold enhancement in the emission ratios. The fluorescence response toward Hg^{2+} or $MeHg^{+}$ by **ATC-Hg** (5 μM) exhibited outstanding linear relationship (Fig. S3, ESI, R^2 = 0.9908 and 0.9956, for Hg^{2+} and $MeHg^{+}$, respectively) between the emission ratios (I_{572}/I_{492}) and the concentration of Hg^{2+} (0-5 μM, 0-1.0 eq.) or $MeHg^{+}$ (0-1 mM, 0-200 eq.). The theoretical lowest detection limit (LOD = 3σ / s) was 27 nM and 5.8 μM for Hg^{2+} and $MeHg^{+}$, respectively.

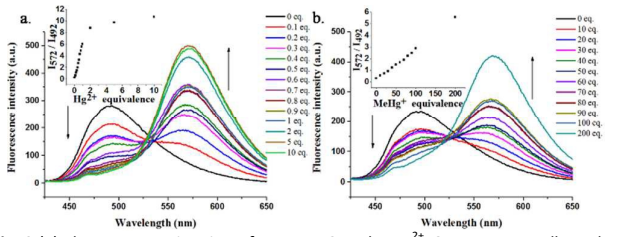

Fig. 2 (a) Fluorescence titration of 5 μM **ATC-Hg** by Hg^{2+}. Spectra was collected 4 min after Hg^{2+} addition. Inset: dose-dependent enhancement of the emission ratios (I_{572}/I_{492}) with respect to Hg^{2+} equivalence. (b) Fluorescence emission titration of 5 μM **ATC-Hg** by $MeHg^{+}$. Spectra was collected 30 min after $MeHg^{+}$ addition. Inset: dose-dependent enhancement of the emission ratios (I_{572}/I_{492}) with respect to $MeHg^{+}$ equivalence. slit: 5 nm/5 nm.

The optical sensing properties of chemosensor are mainly dominated by the specificity of chemical reaction between dosimeter molecule and target species. The selectivity of **ATC-Hg** toward common metal cations, including Ba^{2+}, Cd^{2+}, Co^{2+}, Cr^{3+}, Cu^{2+}, Fe^{3+}, Fe^{2+}, Mn^{2+}, Ni^{2+}, Pb^{2+}, Zn^{2+}, Hg^{2+} in PBS buffer (10 mM, pH 7.4), and Ag^{+} in pure H_2O, was systematically investigated. As shown in Fig. S4 (ESI), the fluorescence response of **ATC-Hg** toward different competitive cations exhibited only negligible changes, except for Cu^{2+}、Mn^{2+} and Ag^{+}. The reason that Cu^{2+} and Mn^{2+} can partly quenching the fluorescence of **ATC-Hg** may come from their coordination with **ATC-Hg**. Yet Ag^{+} is soft acid with the ability of reacting with the sulfur atom like mercury.[8a, 10] Also, the competition studies were investigated. As shown in Fig. S4b and S4c (ESI), the fluorescence response of **ATC-Hg** toward different competitive cations (10 eq.) in the presence of Hg^{2+} (1 eq.) exhibited only negligible changes, except for Ag^{+}. Remarkably, Mn^{2+} and low concentration of Cu^{2+} also exhibited only slight changes in the emission ratio (I_{572}/I_{492}) as a result of ratiometric effect. Nevertheless, in cases where **ATC-Hg** is used for quantification of $MeHg^{+}$, the presence of high levels of Cu^{2+} and Ag^{+} might cause serious interference.

View Article Online
DOI: 10.1039/C8CC01031E

The responsive mechanism of **ATC-Hg** is based on the previously reported Hg^{2+}-promoted desulfurization of 1,3-dithiolane groups and $MeHg^{+}$ is expected to show a similar chemical reaction [6d]. Therefore, the investigation towards the proposed chemical reaction mechanism were carried out by performing ^{1}H-NMR of the **ATC-Hg** in the absence and presence of 2.4 equiv. of Hg^{2+} (excess). As indicated in Fig. 3, after reacting with excess Hg^{2+}, **ATC-Hg** had completely transformed into equivalent compound **c-ql** and **S-Hg**, the integral ratio of which shows 1:1. In the presence of excess Hg^{2+}, the 1,3-dithiolane signal at 5.25 ppm (H^{1}), 3.00-3.70 ppm (H^{2}) and the amino signal at 6.56 ppm (H^{3}) disappeared, while the new signal of **S-Hg** at 2.55 ppm (H^{2*}, Fig. S5, ESI) appeared. Meanwhile, all the proton signal in aromatic region shifted to downfield, in which we can clearly distinguish the appearance singlet of **c-ql** at 8.83 ppm (H^{1*}), 8.75 ppm (H^{4*}) and 8.94 ppm (H^{7*}). Furthermore, mass spectroscopy (Fig. S6, ESI) confirmed the formation of product **c-ql** through the presence of the peaks at m/z = 319.1446 (calcd. for $[M+H]^{+}$, 319.1447).

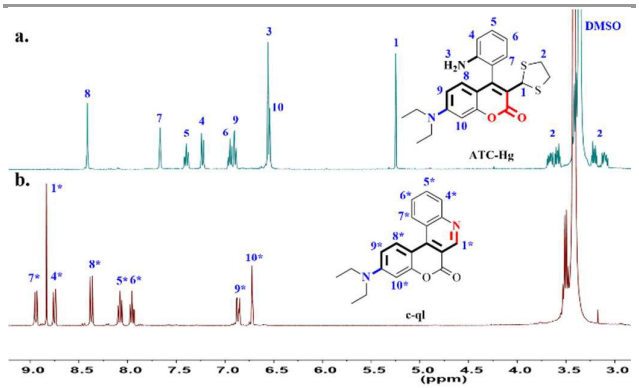

Fig. 3 (a) ^{1}H NMR spectra of **ATC-Hg**, and (b) **ATC-Hg** in the presence of excess Hg^{2+} in DMSO-d_6.

Practical application of **ATC-Hg** in environmental water samples was also investigated. Probe **ATC-Hg** was employed to determine Hg^{2+} concentrations in the water samples from FuNan River. Considering that other components may cause possible interference in real samples, the level of Hg^{2+} in water samples was determined using the standard addition method (often referred to as "spiking" samples) according to previous publications.[11] Added Hg^{2+} in the water samples could be accurately measured with good recovery (Table S1, ESI), indicating that **ATC-Hg** is effective for quantitative detection of Hg^{2+} in real environmental samples.

With the desirable fluorescence properties of **ATC-Hg** for fluorescence detection of Hg^{2+}, the potential application in biological samples was explored. Considering the interference of thiol to Hg(II) in living cells (forming complex) and the high toxicity of Hg^{2+}, we investigated the fluorescence intensity ratio change of **ATC-Hg** in the presence of various concentrations of Hg^{2+} in immobilized HeLa cells. As shown in Fig.4 (D, H, L and P), increasing the concentrations of Hg^{2+}, the fluorescence intensity ratio change of **ATC-Hg**-stained cells could be easily observed. The cells stained by 5 μM **ATC-Hg** alone showed strong fluorescence in the green channel and weaker fluorescence in the red channel. The related ratiometric image of HeLa cells showed an emission ratio of 0.15. In the presence of increased concentrations of Hg^{2+} (5, 10, 25μM), the related emission ratio increased to 0.33 gradually (Fig. S7a, ESI). The fluorescence intensity ratio change of **ATC-Hg**-stained cells showed positive correlation with the concentrations of Hg^{2+}. These results indicated **ATC-Hg** could be used for the detection of Hg(II) in cells, which is of considerable significance for reaction-based fluorescent probes.

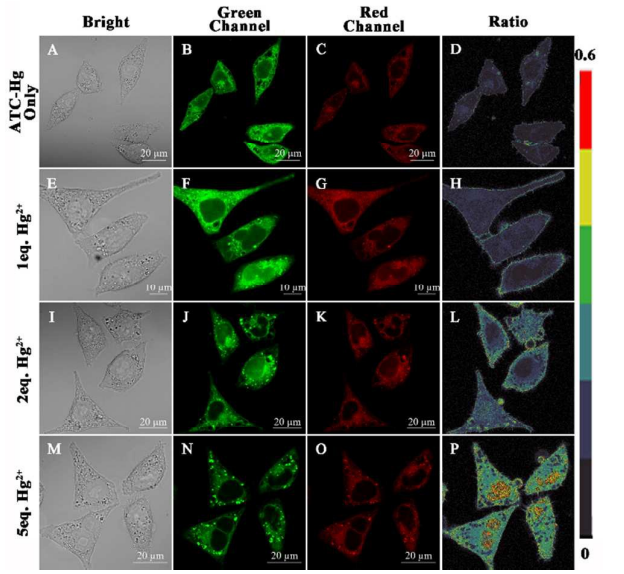

Fig. 4 Fluorescent confocal microscopy images of immobilized HeLa cells stained with 5 μM **ATC-Hg** for 5 min in the presence of various concentrations of Hg^{2+} (5, 10, 25μM) at 37°C. Green channel: 470-520 nm; Red channel images: 560-590 nm; Ratio images of red/green. ex: 405 nm.

It has been reported that the Hg^{2+} could be transformed to $MeHg^{+}$ in some bacteria [12], therefore, fluorescence detection of Hg^{2+} in bacteria would be helpful to understand this transformation and mechanism. To further explore its application, we performed determination of Hg^{2+} with **ATC-Hg** in *E. coli* by imaging on confocal laser scanning microscopy. As illustrated in Fig. 5 and Fig. S7b (ESI), the *E. coli* stained by 5 μM **ATC-Hg** alone showed strong fluorescence in the green channel and weak fluorescence in the red channel. In the presence of increased concentrations of Hg^{2+} (5, 10, 25, 50, 100μM), the fluorescence in the red channel became stronger, and the related emission ratio increased from 0.21 to 0.86 gradually (Fig. S7c, ESI). This showed good positive correlation between the fluorescence intensity ratio change of **ATC-Hg**-stained *E. coli* and the concentrations of Hg^{2+}. These results proved **ATC-Hg** could be applied in tracing Hg^{2+} in *E. coli*, which would be a good tool to study the biotransformation of Hg(II) in bacteria.

View Article Online
DOI: 10.1039/C8CC01031E

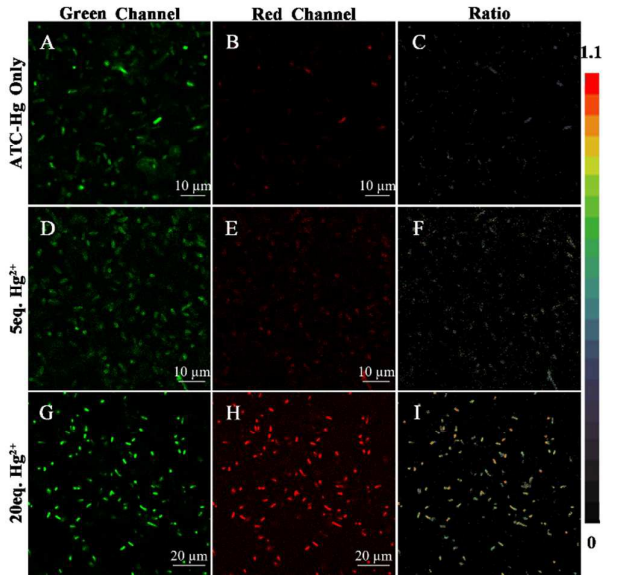

Fig. 5 Fluorescent confocal microscopy images of normal *E. coli* stained with 5 μM **ATC-Hg** for 5 min in the presence of various concentrations of Hg^{2+} (0, 25, 100μM) for 30 min in the shaker at 37°C. Green channel images: 470-520 nm; Red channel images: 560-590 nm; Ratio images of red/green. ex: 405 nm.

Conclusions

In summary, a novel reaction-based fluorescent probe (**ATC-Hg**) was designed and synthesized for the quantification of Hg^{2+} and $MeHg^{+}$ *via* the "covalent assembly" principle. Significantly, probe **ATC-Hg** exhibits high sensitivity and selectivity towards Hg^{2+} and $MeHg^{+}$, the theoretical lowest detection limit of Hg^{2+} and $MeHg^{+}$ is 27 nM and 5.8 μM, respectively. Meanwhile, the responsive mechanism was proved by HRMS, ^{1}H NMR spectrum. Moreover, **ATC-Hg** was successfully applied to quantitative detection of Hg^{2+} in real environmental samples and imaging of Hg^{2+} both in HeLa cells and *E. coli*. We anticipate this probe should prove useful for Hg^{2+} determination in biosamples.

Acknowledgements

This work was financially supported by the National Natural Science Foundation of China (nos 21572147, 21232005 and J1103315).

Notes and references

1 Y.-M. Yang, Q. Zhao, W. Feng, and F.-Y. Li, *Chem. Rev.*, 2013, **113**, 192-270.
2 (a) R. Eisler, *Mercury Hazards to Living Organisms*, CRC Press, New York, 2006; (b) M. Aschner, N. Onishchenko and S. Ceccatelli, *Toxicology of Alkylmercury Compounds*, in *Organometallics in Environment and Toxicology: Metal Ions in Life Sciences*, ed. A. Sigel, H. Sigel and R. K. O. Sigel, 2010, vol. 7, ch. 12, p. 403.
3 (a) A. Aliberti, P. Vaiano, A. Caporale, M. Consales, M. Ruvo, A. Cusano, *Sens. Actuators B*, 2017, **247**, 727–735; (b) L.-Y. Zong, Y.-J. Xie, Q.-Q. Li, Z. Li, *Sens. Actuators B*, 2017, **238**, 735–743; (c) W.-Y. Fang, G.-B. Zhang, J. Chen, L. Kong, L.-M. Yang, H. Bi, J.-X. Yang, *Sens. Actuators B*, 2016, **229**, 338–346; (d) I. Kim, N.-E. Lee, Y.-J. Jeong, Y.-H. Chung, B.-K. Cho and E. Lee, *Chem. Commun.*, 2014, **50**, 14006; (e) L. Feng, W. Shi, J.-C. Ma, Y.-B. Chen, F. Kui, Y.-H. Hui, Z.-F. Xie, *Sens. Actuators B*, 2016, **237**, 563–569; (f) L.-Y. Zong, C. Wang, Y.-C. Song, Y.-J. Xie, P. Zhang, Q. Peng, Q.-Q. Li, Z. Li, *Sens. Actuators B*, 2017, **252**, 1105–1111; (g) S.-S. Zhang, Q.-F. Niu, L.-X. Lan, T.-D. Li, *Sens. Actuators B*, 2017, **240**, 793–800; (h) P. Srivastava, S. S. Razi, R. Ali, R. C. Gupta, S. S. Yadav, G. Narayan, and A. Misra, *Anal. Chem.*, 2014, **86**, 8693-8699; (i) A. Kumar, P. S. Chae, *Sens. Actuators B*, 2017, **251**, 416–426; (j) L. N. Neupane, E.-T. Oh, H. J. Park, and K.-H. Lee, *Anal. Chem.*, 2016, **88**, 3333-3340.
4 Y.-Y. Lv, W. Gu, J.-B. Wang, W.-B. Huang, W.-X. Shen, X.-Y. Sun, *Sens. Actuators B*, 2017, **246**, 1017–1024.
5 (a) Y.-C. Chen, W.-J. Zhang, Y.-J. Cai, Ryan T. K. Kwok, Y.-B. Hu, J. W. Y. Lam, X.-G. Gu, Z.-K. He, Z. Zhao, X.-Y. Zheng, B. Chen, C. Gui and B.-Z. Tang, *Chem. Sci.*, 2017, **8**, 2047–2055; (b) Y. Zhou, X.-F. He, H. Chen, Y. Wang, S.-Z. Xiao, N.-N. Zhang, D.-J. Li, K.-B. Zheng, *Sens. Actuators B*, 2017, **247**, 626–631; (c) Y. Jiao, X. Liu, L. Zhou, H.-Y. He, P. Zhou, C.-Y. Duan, *Sens. Actuators B*, 2017, **247**, 950–956; (d) J.-W. Hu, Z.-J. Hu, S. Liu, Q. Zhang, H.-W. Gao, K. Uvdal, Sens. Actuators B, 2016, **230**, 639–644; (e) J.-X. Ru, X. Chen, L.-P. Guan, X.-L. Tang, C.-M. Wang, Y. Meng, G.-L. Zhang, and W.-S. Liu, *Anal. Chem.*, 2015, **87**, 3255-3262.
6 (a) K. Bera, A. K. Das, M. Nag, and S. Basak, *Anal. Chem.*, 2014, **86**, 2740-2746; (b) H.-B. Xiao, Y.-Z. Zhang, S.-Z. Li, W. Zhang, Z.-Y. Han, J.-J. Tan, S.-Y. Zhang, J.-Y. Du, *Sens. Actuators B*, 2016, **236**, 233–240; (c) M.-Y. She, S.-P. Wu, Z.-H. Wang, S.-Y. Ma, Z. Yang, B. Yin, P. Liu, S.-Y. Zhang, J.-L. Li, *Sens. Actuators B*, 2017, **247**, 129–138; (d) Z.-Q. Zhang, B.-Y Zhang, X.-H. Qian, Z. Li, Z.-P. Xu, and Y.-J. Yang, *Anal. Chem.*, 2014, **86**, 11919-11924; (e) L.-L Song, Z.-H. Lei, B.-Y. Zhang, Z.-P. Xu, Z. Li and Y.-J. Yang, *Anal. Methods*, 2014, **6**, 7597–7600; (f) M.-M. Hong, X.-Y. Lu, Y.-H. Chen, D.-M. Xu, *Sens. Actuators B*, 2016, **232**, 28–36; (g) J.-L. Wang, W.-L. Li, L.-P. Long, *Sens. Actuators B*, 2017, **245**, 462–469.
7 C.-J. Wu, J.-B. Wang, J.-J. Shen, C. Bi, H.-W. Zhou, *Sens. Actuators B*, 2017, **243**, 678–683.
8 (a) H.-R. Yang, C.-M. Han, X.-J. Zhu, Y. Liu, K. Y. Zhang, S.-J. Liu, Q. Zhao, F.-Y. Li, and W. Huang, *Adv. Funct. Mater.*, 2016, **26**, 1945–1953; (b) M. Deng, D.-Y. Gong, S.-C. Han, X.-T. Zhu, A. Iqbal, W.-S. Liu, W.-W. Qin, H.-C. Guo, *Sens. Actuators B*, 2017, **243**, 195–202; (c) B. Díaz de Greñu, J. García-Calvo, J. Cuevas, G. García-Herbosa, B. García, N. Busto, S. Ibeas, T. Torroba, B. Torroba, A. Herrerab and S. Pons, *Chem. Sci.*, 2015, **6**, 3757–3764; (d) J. García-Calvo, S. Vallejos, F. C. García, J. Rojo, J. M. García and T. Torroba, *Chem. Commun.*, 2016, **52**, 11915–11918; (e) Y. Liu, S. Wang, Y. Ma, J. Lin, H.-Y. Wang, Y.-Q. Gu, X.-Y. Chen, and P. Huang, *Adv. Mater.*, 2017, **29**, 1606129; (f) G. Singh, K.-M. Hsu, Y.-J. Chen, S.-C. Wu, C.-Y. Chen and Y.-M. Wang, *Chem. Commun.*, 2015, **51**, 12032–12035; (g) Y. Liu, M. Chen, T.-Y. Cao, Y. Sun, C.-Y. Li, Q. Liu, T.-S. Yang, L.-M. Yao, W. Feng, and F.-Y. Li, *J. Am. Chem. Soc.*, 2013, **135**, 9869-9876; (h) D.-S. Mei, B.-K. He, L. Chen, Z.-J. Yao, *Tetrahedron Letters*, 2012, **53**, 3463–3466; (i) H. Wang and W.-H. Chan, *Tetrahedron*, 2007, **63**, 8825–8830.
9 (a) M.-Y. Wu, K. Li, C.-Y. Li, J.-T. Hou and X.-Q. Yu, *Chem. Commun.*, 2014, **50**, 183-185; (b) J.-T. Hou, J. Yang, K. Li, Y.-X. Liao, K.-K. Yu, Y.-M. Xie and X.-Q. Yu, *Chem. Commun.*, 2014, **50**, 9947-9950; (c) M.-Y. Wu, K. Li, Y.-H. Liu, K.-K. Yu, Y.-M. Xie, X.-D. Zhou, X.-Q. Yu, *Biomaterials*, 2015, **53**, 669-678.
10 R. G. Pearson, *J. Am. Chem. Soc.*, 1963, **85**, 3533.
11 (a) W.-Y. Lin, L.-L. Long and W. Tan, Chem. Commun., 2010, 46, 1503-1505; (b) J. Li, C.-F. Zhang, S.-H. Yang, W.-C. Yang, and G.-F. Yang, Anal. Chem. 2014, 86, 3037-3042.
12 (a) J. M. Parks, A. Johs, M. Podar, R. Bridou, R. A. Hurt Jr., S. D. Smith, S. J. Tomanicek, Y. Qian, S. D. Brown, C. C. Brandt, A. V. Palumbo, J. C. Smith, J. D. Wall, D. A. Elias, L.-Y. Liang, *Science*, 2013, **339**, 1332-1335; (b) H.-Y. Hu, H. Lin, W. Zheng, S. J. Tomanicek, A. Johs, X.-B. Feng, D. A. Elias, L.-Y. Liang and B.-H. Gu, *Nature Geosci.*, 2013, **6**, 751-754.

View Article Online
DOI: 10.1039/C8CC01031E

A reaction-based ratiometric fluorescent sensor for detection of Hg(II) ions both in cells and bacteria

Sheng-Lin Pan, Kun Li, Ling-Ling Li, Meng-Yang Li, Lei Shi, Yan-Hong Liu and Xiao-Qi Yu

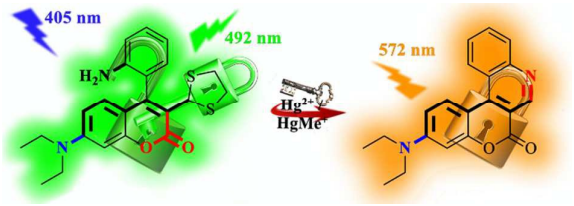

A novel reaction-based fluorescent probe *via* "covalent assembly" principle was presented and successfully applied for imaging of Hg(II) in HeLa cells and E. coli.